ENHANCING TEMPERATURE STABILITY OF LAMÉ-MODE SILICON RESONATOR USING ELASTIC NONLINEARITY

Dicheng Mo, Shaurya Dabas, Banafsheh Jabbari, and Roozbeh Tabrizian
Department of Electrical and Computer Engineering, University of Florida, USA

ABSTRACT

This paper reports on the use of elastic nonlinearity for compensation of the second-order temperature coefficients of frequency (TCF_2) in a piezoelectrically transduced Lamé mode resonator implemented in degenerately n-doped single crystal silicon (Si). For the first time, we are demonstrating a resonator with a third-order polynomial temperature characteristic of frequency through significant reduction of the $|TCF_2|$ from 78 $ppb/°C^2$ to 9.7 $ppb/°C^2$. This is achieved by the use of elastic nonlinearity in Si that induces a positive frequency duffing (*i.e.*, stiffening) upon exciting the resonator into large vibration amplitudes when the temperature deviates from the intrinsic turn-over point. The resonator is created in a 50µm-thick Si layer with a resistivity of $0.002\ \Omega.cm$, and a $600nm$-thick piezoelectric aluminum-scandium nitride ($Al_{0.7}Sc_{0.3}N$) transducer is used to excite a cross-sectional Lamé mode with quadratic temperature characteristic of frequency when operating in linear elastic regime. An integrated resistor, connected to the resonator body, is used to accurately monitor the local temperature. This temperature is then used to control the loop gain of an oscillator created around the resonator, to induce nonlinear stiffening upon deviation from turn-over temperature, resulting in analytical control over temperature characteristic and substantial reduction of *TCF₂*.

KEYWORDS

Lamé resonator, oven-controlled crystal oscillator, stable clock, temperature coefficients of frequency, elastic nonlinearity.

INTRODUCTION

Oven-controlled crystal oscillators (OCXO) are ubiquitous in compact defense and consumer electronic systems that require clock holdover between synchronization events or during GPS denial scenarios. OCXOs rely on quartz [1-4] or Si [5-8] mechanical resonators that provide temperature characteristics with a local extremum, known as turn-over temperature (T_{TO}), where the linear temperature coefficient of frequency (TCF_1) is nulled. Assuming a third-order polynomial temperature characteristic of the resonator, T_{TO} can be derived from TCF_is through:

$$T_{TO} = \frac{-2TCF_2 + \sqrt{4TCF_2^2 - 12TCF_1TCF_3}}{6TCF_3} \quad (1).$$

When T_{TO} is higher than operational temperature range (*e.g.*, -40°C to 85°C in consumer electronics applications), ovenization at such temperature enables frequency stabilization that is limited by higher-order temperature coefficients (*i.e.*, TCF_2 and TCF_3) and temperature instability of the resonator (ΔT_{error}). Assuming an ovenization apparatus that controls resonator temperature over $T_{TO} \pm \Delta T_{error}$, frequency drift of the OCXO is derived from:

$$\left(\frac{\Delta f}{f_0}\right)_{OCXO} = \{TCF_2\Delta T_{error}^2 \pm TCF_3\Delta T_{error}^3\}_{max} \quad (2).$$

It is worth noting that TCF_2 and TCF_3 are fundamental merits set by the finite and inherent temperature dependence of elasticity, density, and dimensions of the resonator. Therefore, to improve OCXO's frequency stability, the only degree of design freedom is $\Delta T_{instability}$ that can be reduced through increasing thermal gain of

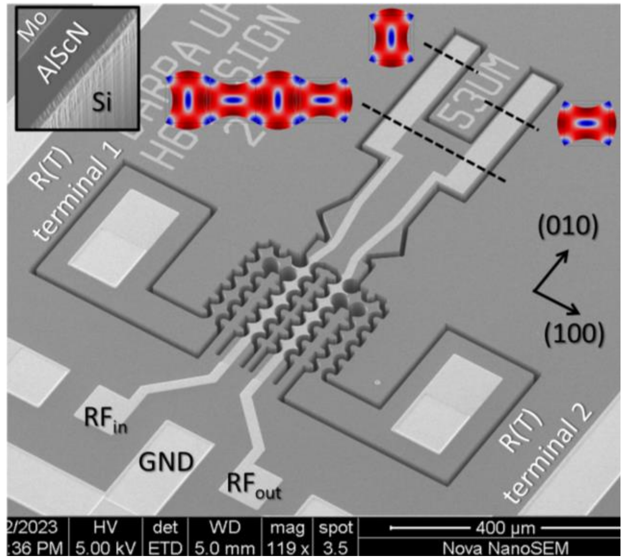

Figure 1: SEM image of the AlScN-on-Si cross-sectional Lamé mode resonator. The inset shows the resonator stack details. The Si body is highly n-doped (0.002 ohm.cm). Energy localization is achieved through dispersion engineering and phononic crystals (PnC). Two PnCs, in series, are used as temperature sensing resistance.

the oven (*i.e.*, scaling factor of ambient temperature to resonator local temperature). Assuming an ideal resonator temperature sensing scheme, with infinitesimally small error, OCXO's thermal gain can be increased indefinitely through proper thermal isolation of OCXO package and consumption of sufficiently large ovenization power. Current quartz and Si OCXOs consume over 0.5-5 Watts of power to achieve sub part per billion (ppb) temperature stability.

However, emerging applications such as new wireless generations and tactical missions require ultra-stable clocks that fulfill Stratum-2 hold-over requirements (*i.e.*, less than 10^{-11} frequency drift). Stratum-1 clocks would be essential to enable wireless systems to meet latency requirement for Next G, over long periods of GPS-denial incidents. To achieve Stratum-1 performance, the frequency stability of the resonator should be within one ppt (*i.e.*, one part in 10^{12}) over -40°C to 85°C temperature range. Such requirement translates to an extremely small ΔT_{error} and unrealistically large volume and power consumption of OCXO. Therefore, a fundamental approach that targets device-level, and ideally analytically controlled, reduction of TCF_2 and TCF_3 is essential to enable realization of chip-scale low-power Stratum-1 mechanical clocks.

In this paper, we demonstrate a novel approach for analytical compensation of higher-order temperature coefficients of frequency in an AlScN-on-Si resonator operating in cross-sectional Lamé (X-Lamé) mode (Fig. 1). In this approach, the large elastic nonlinearity of degenerately n-doped Si and corresponding amplitude-controlled frequency duffing of the X-Lamé resonator is used to compensate the large $|TCF_2|$ by nearly an order of magnitude.

CONCEPT

In presence of elastic nonlinearities, Lamé mode resonator's motion is governed by a nonlinear differential equation:

$$M_{eq}\ddot{u} + D_{eq}\dot{u} + K_{eq,0}u + K_{eq,2}u^3 = F_{piezo} \quad (3).$$

Here, u is resonator displacement magnitude. M_{eq} and D_{eq} are equivalent mass and damping of the resonator. $K_{eq,0}$ and $K_{eq,2}$ are first- and third-order equivalent spring constants, and F_{piezo} is the equivalent force exerted by the AlScN piezoelectric transducer.

When u is analytically controlled to provide a desirable temperature dependency, *i.e.*,

$$u(T) = u_0 + AT + BT^2 \quad (4).$$

where A and B are desirable factors enforced through temperature-to-input power scaling factor, the temperature characteristic of the resonator in nonlinear regime is governed by:

$$f \cong f(0)\left[1 + TCF_{NL,1}T + TCF_{NL,2}T^2 + TCF_{NL,3}T^3\right] \quad (5).$$

Here, the nonlinear temperature coefficients are driven as:

$$\begin{cases} TCF_{NL,1} = TCF_1 + 2\kappa u_0 A \\ TCF_{NL,2} = TCF_2 + \kappa A^2 + 2\kappa u_0 B \\ TCF_{NL,3} = TCF_3 + 2\kappa AB \end{cases} \quad (6).$$

Therefore, opting for proper A and B values, one can compensate for higher-order temperature coefficients of frequency. For practical implementation of this concept, resonator temperature is monitored based on real-time resistance measurement of the n-doped Si phononic crystal (PnC) tether. This information is used to control the input power (P_{in}) of the resonator through proper scaling factor, facilitating the use of nonlinear duffing for compensation of higher-order temperature coefficients of frequency. For this purpose, COMSOL and MATLAB models are developed to quantify frequency duffing for different drive voltages (Fig. 2) and optimize scaling factor targeting compensation of the large TCF_2 of X-Lamé resonator.

DESIGN AND MODELING

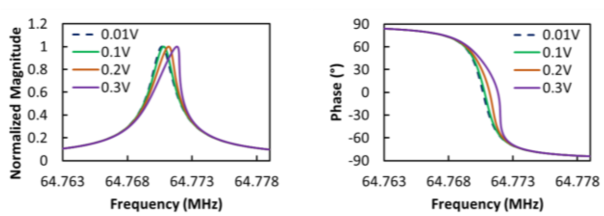

Figure 2: Normalized vibration amplitude upon various derive voltages, extracted using COMSOL and MATLAB models.

The X-Lamé mode resonator in this work utilizes a $50\mu m$ degenerately phosphorous-doped Si device layer, with a $600nm\ Al_{0.7}Sc_{0.3}N$ layer grown atop to couple the electrical excitation with the mechanical deformation. This width-extensional stress present on the top surface of the square Si body contributes to the excitation of the cross-sectional Lamé mode.

To minimize the dissipation and enhance the quality factor (Q), the resonator geometry and material stack are optimized for efficient energy localization of the X-Lamé mode as well as reduction of thermoelastic dissipation [9][10]. Further, the resonator is connected to the substrate through PnC anchors to further enhance Q. Besides the PnC tethers that host electrode routings for the two ports, two additional tethers are also used to enable monitoring resonator local temperature by continuously measuring their temperature-dependent resistance, $R(T)$. This information is then used to control the vibration amplitude of the resonator through autonomous variation of oscillator loop gain.

Merited from the high Q of the resonator, the large elastic nonlinearity of n-doped Si, and the efficient piezoelectric coupling of $Al_{0.7}Sc_{0.3}N$, the displacement magnitude u_0 of the X-Lamé mode is sufficiently large for nonlinear operation with relatively small drive voltage (or equivalently input power). According to the governing nonlinear equation of motion for the X-Lamé resonator, with an increasing u_0, the third-order equivalent spring constant growingly affect the frequency response, inducing a positive duffing due to resonator stiffening. Accordingly, it is possible to compensate for the TCF_i by exploiting a vibration amplitude with a properly engineered temperature dependence and optimizing the nonlinear temperature coefficients $TCF_{NL,i}$.

FABRICATION PROCESS

Figure 3 illustrates the fabrication process flow for realization of the AlScN-on-Si X-Lamé resonator. Utilizing reactive magnetron sputtering from Evatec sputtering tool, a highly crystalline c-axis orientated ~600nm-thick $Al_{0.7}Sc_{0.3}N$ is deposited atop a $\sim 50\mu m$-thick highly phosphorous-doped Silicon device layer of the SOI wafer. Atop of the $Al_{0.7}Sc_{0.3}N$ layer a 50nm molybdenum (Mo) is deposited by DC sputtering and patterned using SF_6 based reactive-ion-etching inductively coupled plasma (RIE-ICP) to form the top electrode, followed by Cl_2 based $Al_{0.7}Sc_{0.3}N$ dry etch to form the electrical access to the low-resistivity Si layer that serves as the bottom electrode.

Next, the routings and pads are outlined by 300nm platinum (Pt) lift-off to establish proper electrical access to the top Mo electrodes and bottom Si layer, followed by resonator lateral dimension definition using high aspect-ratio deep reactive-iron-etching (DRIE) through the $50\mu m$ Si device layer to the buried silicon oxide (SiO_2) layer. The DRIE is strictly timed to avoid Si over-etch around the Si and oxide layer interface, and the sidewall polymer residue of the Bosch DRIE process is cleaned by ashing.

Lastly, the Si handle layer under the resonator is etched from backside using DRIE to reach the buried SiO_2 layer, followed by the selective SiO_2 removal to release the device. The selectivity of Si and SiO_2 recipe ensured a flat resonator bottom surface profile.

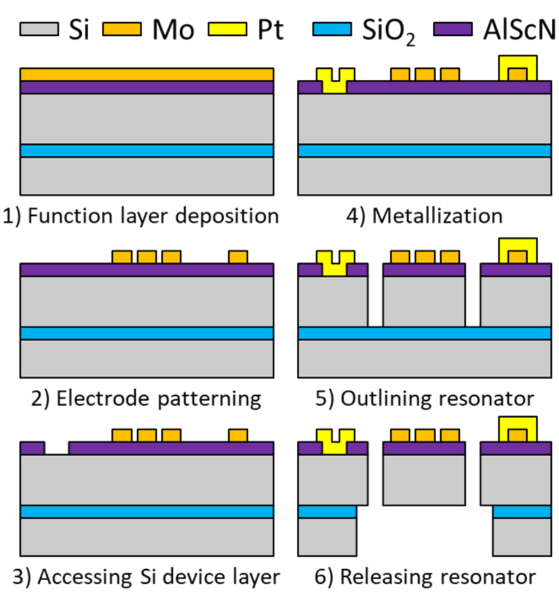

Figure 3: Fabrication process for realization of AlScN-on-Si cross-sectional Lamé mode resonator.

CHARACTERIZATION

The AlScN-on-Si X-Lamé resonator is wire-bonded to designated PCB board and contained within a vacuum chamber with pressure lower than 5e-5 mbar, electrically accessed through multiple RF cables. An environmental chamber is used to provide temperature sweeps to enable extraction of temperature characteristics. The frequency response of the resonator is measured using a Keysight 5222A PNA Network Analyzer. The resonator is locked to oscillation and its frequency is tracked using the phase lock loop and frequency counter functions integrated within a Zurich UHF lock-in amplifier.

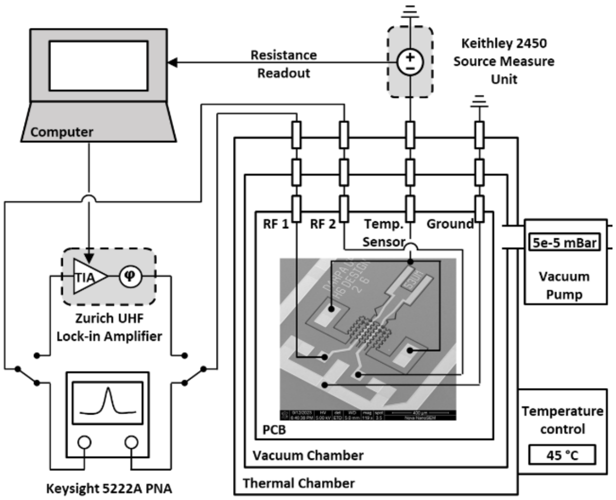

Figure 4: Test-setup for characterizing the S_{21} in nonlinear regime and identification of $P_{in}(T)$ for TCF$_i$ compensation.

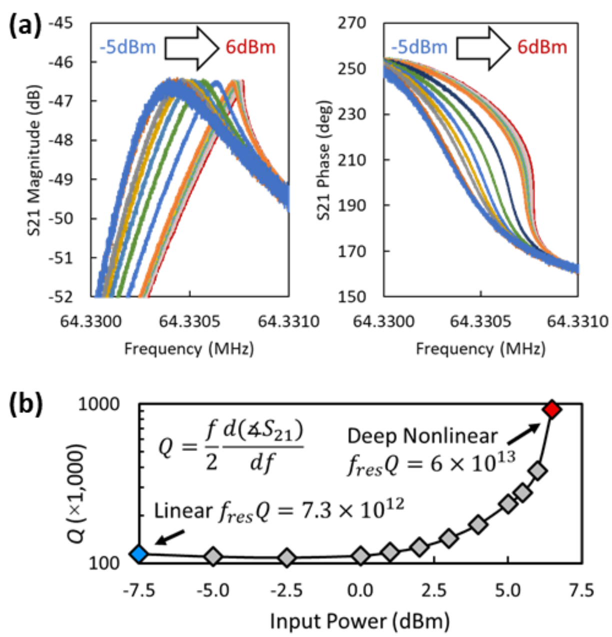

Figure 5: (a) Measured S_{21} of the resonator for different input powers. The evolution of S_{21} amplitude and gain is shown. The nonlinear stiffening of the resonator results in forward duffing and increased frequency. This nonlinearity-induced drift is used for compensation of TCF$_2$. (b) Measured Q of the resonator for different input powers, showing an order of magnitude increase when the resonator is operating in nonlinear regime.

Resonator Nonlinearity Characterization

The measurement setup for analytical control and characterization of resonator temperature characteristic in nonlinear regime is shown in Fig. 4. The resonator frequency response is monitored using continuous sweeps by VNA, with an input power level that is controlled over -5dBm to 6dBm. Figure 5 (a) shows the measured magnitude and phase of resonator's transmission responses (S_{21}) for different input powers, highlighting a maximum achievable frequency drift of 5.75ppm, before entering the bistability regime, merited from the elastic nonlinearity of highly n-doped Si when the resonator is driven by ~6dBm input power. By controlling the temperature dependence of the input power, through an autonomous feedback, this positive duffing is used to compensate resonator's TCf_is. Figure 5 (b) shows the resonator Q, extracted from its phase across different input power, highlighting a favorable boost as gradually entering into nonlinear regime. While the PnC anchoring tethers provide optimized acoustic energy localization required for resonator high Q operation, driving the resonator into nonlinearity further improves the Q, which positively contributes to improve oscillator's short-term stability.

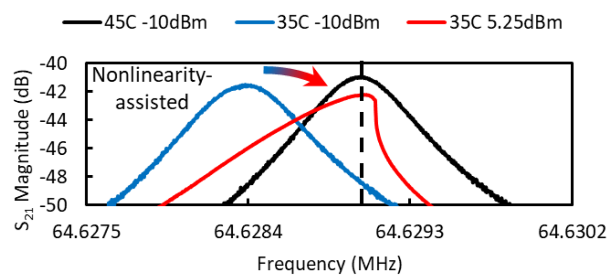

Figure 6: Experimental demonstration of nonlinearity-assisted temperature compensation concept. Temperature reduction from turn-over (45°C) to 38°C results in frequency reduction, when operating in linear regime. Application of higher input power of 5.25 dBm at 38°C enables pulling the frequency back to turn-over frequency.

Temperature Characterization

To determine the required input power for nonlinearity-assisted compensation at different temperature, linear resonator S_{21} at different temperatures is first measured and compared with S_{21} at T_{TO}, followed by increasing the input power to identify the required value to minimize the temperature-induced frequency drift by nonlinear duffing. Figure 6 shows the experimental result highlighting a 5.25dBm input power required to fully compensate the frequency drift induced by a $10°C$ temperature deviation from the $T_{TO} \approx 45°C$.

For a closed-loop temperature compensation, acquiring the resonator temperature is necessary to determine the input power magnitude, which is achieved by measuring the resistance of the highly n-doped Si PnC body attached to the X-Lamé resonator. Based on open loop characterization and identification of required input power at each temperature, a closed-loop nonlinearity-assisted compensation setup with autonomous control of vibration amplitude is developed as shown in Fig. 7 (a). In this setup, resonator temperature is monitored using real-time resistance readout and translated by the previously extracted temperature-resistance characteristic, followed by scripting oscillator loop-gain through a desired polynomial function. Figure 7 (b) shows the measured temperature characteristic of the oscillator over $30° - 50°C$, in linear regime with constant resonator P_{in} = -5 dBm. This is compared with the temperature characteristic in nonlinear regime

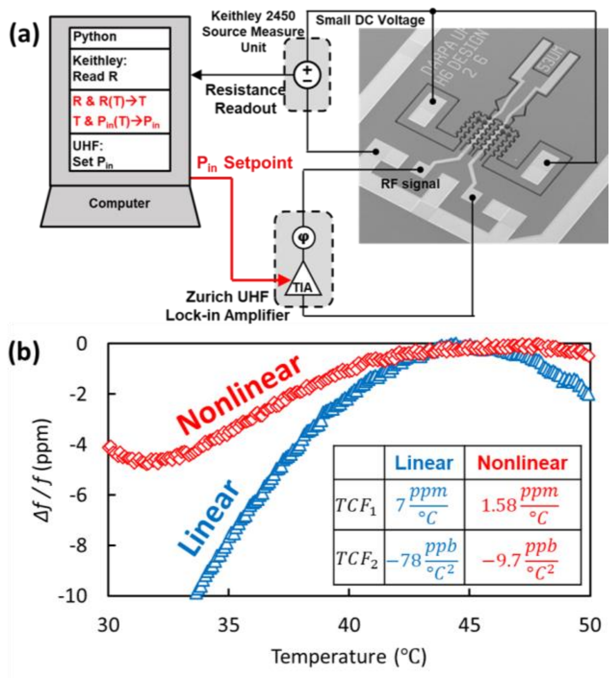

Figure 7: (a) The autonomous setup for realization of nonlinearity assisted temperature stable oscillator. A lock-in amplifier is used to create oscillations using the nonlinear resonator. The gain-loop is automatically controlled, based on the measured temperature-dependent resistance attached to the resonator. (b) Measured temperature characteristic of the oscillator in linear & nonlinearity-assisted regimes, using the setup shown in fig. 6. The inset table shows the TCF_i values in the two regimes, highlighting ~8 times reduction of $|TCF_2|$.

with closed-loop control of the P_{in}. While sustaining the T_{TO} at the same temperature, the autonomous nonlinear compensation enabled an order of magnitude reduction in resonator $|TCf_2|$, from -78 ppb/°C^2 to -9.7 ppb/°C^2. Such a reduction provided a nearly flat temperature characteristic that is well suited for realization of OCXO with significantly relieved constraint on ΔT_{error}, which translates to lower power consumption and volume of the clock. This demonstration highlights the potential of this approach to realize ultra-stable chip-scale clocks towards fulfilling Stratum-1 level holdover requirements of emerging electronic systems.

CONCLUSION

This paper, for the first time, demonstrates the temperature compensation technique utilizing the elastic nonlinearity in the AlScN-on-Si X-Lamé mode resonator. The stiffening effect due to the heavily phosphorus-doped Si contributes to a positive frequency shift that can balance the deviation due to the temperature offset. Besides, to decide the input power level for proper decision of stiffening, the resonator temperature is real-time translated by monitoring the resistance of PnC, which also contributes to suppressing the support loss and maximizing the Q. Experiential characterization of S_{21} reports a 5.75ppm positive frequency shift when entering nonlinear regime, with a significant Q improvement exceeding the Si $f_{res} \times Q$ limit observed. Furthermore, the compensation for $10°C$ temperature offset from the T_{TO} around $45°C$ is accomplished utilizing the duffing effect at 5.25dBm input power, and based on the required P_{in} and PnC resistance value across the interested temperature range, a closed-loop control of the amplifier gain is scripted to provide sufficient input power for positive frequency shift that compensates for the deviation at this temperature. Lastly, the temperature-compensated oscillator with closed-loop gain control is implemented using a Zurich Lock-in amplifier and Keithley 2450 Source Measurement Unit. While sustaining the T_{TO} at approximately the same temperature, nearly one order of magnitude improvement in $|TCF_2|$ is achieved by exploiting elastic nonlinearity, highlighting the potential of this approach to realize ultra-stable clocks with relaxed temperature-isolation and ovenization requirements.

ACKNOWLEDGEMENTS

This work was sponsored by the Defense Advanced Research Project Agency H6 program under Contract No. HR00112390018. The authors would like to thank the University of Florida Nano Research Facility cleanroom staff for their technical support.

REFERENCES

[1] J. R. Vig, "Introduction to Quartz Frequency Standards. Revision." NASA STI/Recon Tech. Report N93 (1992): 15330.

[2] W. -L. Hsieh, W. -C. Wang, E. -S. Hsu, S. -H. Kao and M. -H. Wang, "The World's Smallest Quartz-Based OCXO for 5G Synchronization Applications," *2021 Joint Conference of the European Frequency and Time Forum and IEEE International Frequency Control Symposium (EFTF/IFCS)*, Gainesville, FL, USA, 2021, pp. 1-4.

[3] B. Long and G. Weaver, "Quartz crystal oscillators with direct resonator heating," *45th Annual Symposium on Frequency Control*, Los Angeles, CA, USA, 1991, pp. 384-392.

[4] J. Lim, K. Choi, H. Kim, T. Jackson and D. Kenny, "Miniature Oven Controlled Crystal Oscillator (OCXO) on a CMOS Chip," IEEE *International Frequency Control Symposium and Exposition*, Miami, FL, USA, 2006, pp. 401-404.

[5] A. Partridge, H. -C. Lee, P. Hagelin and V. Menon, "We know that MEMS is replacing quartz. But why? And why now?," *2013 Joint European Frequency and Time Forum & International Frequency Control Symposium (EFTF/IFC)*, Prague, Czech Republic, 2013, pp. 411-416.

[6] H. -K. Kwon, L. C. Ortiz, G. D. Vukasin, Y. Chen, D. D. Shin and T. W. Kenny, "An Oven-Controlled MEMS Oscillator (OCMO) With Sub 10mw, ± 1.5 PPB Stability Over Temperature," *2019 20th International Conference on Solid-State Sensors, Actuators and Microsystems & Eurosensors XXXIII (TRANSDUCERS & EUROSENSORS XXXIII)*, Berlin, Germany, 2019, pp. 2072-2075.

[7] C. -S. Liu, R. Tabrizian and F. Ayazi, "A ±0.3 ppm Oven-Controlled MEMS Oscillator Using Structural Resistance-Based Temperature Sensing," in *IEEE Transactions on Ultrasonics, Ferroelectrics, and Frequency Control*, vol. 65, no. 8, pp. 1492-1499, Aug. 2018.

[8] R. Tabrizian, A. Daruwalla, and F. Ayazi. "High-Q energy trapping of temperature-stable shear waves with Lamé cross-sectional polarization in a single crystal silicon waveguide." *Applied Physics Letters* 108.11 (2016).

[9] S. Dabas, D. Mo, B. Chatterjee and R. Tabrizian, "Ultra-High Q Self-Ovenized AlScN-on-Si X-Lamé Resonator for Stable Clock Generation," *2024 IEEE 37th International Conference on Micro Electro Mechanical Systems (MEMS)*, Austin, TX, USA, 2024, pp. 152-155.

CONTACT

*Dicheng Mo, tel: +1-352-328-8369; dicheng.mo@ufl.edu.

*Shaurya Dabas, tel: +1-407-533-1385; shauryadabas@ufl.edu.